International Journal of Computer Assisted Radiology and Surgery (2023) 18:1093–1099
https://doi.org/10.1007/s11548-023-02869-3

ORIGINAL ARTICLE

Robotically controlled three-dimensional micro-ultrasound for prostate biopsy guidance

Reid Vassallo[1] · Tajwar Abrar Aleef[1] · Qi Zeng[2] · Brian Wodlinger[3] · Peter C. Black[4] · Septimiu E. Salcudean[1,2]

Received: 7 February 2023 / Accepted: 7 March 2023 / Published online: 30 March 2023

Abstract

Purpose Prostate imaging to guide biopsy remains unsatisfactory, with current solutions suffering from high complexity and poor accuracy and reliability. One novel entrant into this field is micro-ultrasound (microUS), which uses a high-frequency imaging probe to achieve very high spatial resolution, and achieves prostate cancer detection rates equivalent to multiparametric magnetic resonance imaging (mpMRI). However, the ExactVu transrectal microUS probe has a unique geometry that makes it challenging to acquire controlled, repeatable three-dimensional (3D) transrectal ultrasound (TRUS) volumes. We describe the design, fabrication, and validation of a 3D acquisition system that allows for the accurate use of the ExactVu microUS device for volumetric prostate imaging.

Methods The design uses a motorized, computer-controlled brachytherapy stepper to rotate the ExactVu transducer about its axis. We perform geometric validation using a phantom with known dimensions and compare performance with magnetic resonance imaging (MRI) using a commercial quality assurance anthropomorphic prostate phantom.

Results Our geometric validation shows accuracy of 1 mm or less in all three directions, and images of an anthropomorphic phantom qualitatively match those acquired using MRI and show good agreement quantitatively.

Conclusion We describe the first system to acquire robotically controlled 3D microUS images using the ExactVu microUS system. The reconstructed 3D microUS images are accurate, which will allow for future applications of the ExactVu microUS system in prostate specimen and in vivo imaging.

Keywords Micro-ultrasound · Prostate cancer · Three dimensional · Robotics

Introduction

Prostate cancer (PCa) is the second-most frequently diagnosed cancer in males worldwide, and the World Health Organization estimates that 2020 saw over 1.4 million new diagnoses and 375,000 deaths [1]. The standard diagnostic method for PCa is systematic transrectal ultrasound (TRUS)-guided biopsy, where a series of core needle biopsy samples are obtained [2]. Systematic sampling is required because suspicious prostate lesions cannot be reliably targeted since they often appear isoechoic on standard TRUS B-mode images [3]. This standardized biopsy method has a false negative rate of over 30% [4] because it is unclear whether a negative result is due to not sampling the correct area of the prostate, or if no cancerous cells are present.

Being able to perform targeted biopsies on suspicious lesions would address these limitations, and this can currently be done using multiparametric magnetic resonance imaging (mpMRI) [5]. However, the limitations of mpMRI include high cost, low accessibility, and the inability to acquire images in real-time. To make up for its lack of real-time imaging, MRI-ultrasound (US) fusion systems are used and rely upon registration between the MRI and US images. Although US is usually a two-dimensional (2D) modality, three-dimensional (3D) images can be acquired by mov-

✉ Reid Vassallo
reidvass@student.ubc.ca

1 School of Biomedical Engineering, The University of British Columbia, 251-2222 Health Sciences Mall, Vancouver, BC V6T 1Z3, Canada

2 Department of Electrical and Computer Engineering, The University of British Columbia, 5500-2332 Main Mall, Vancouver, BC V6T 1Z4, Canada

3 Exact Imaging, 15-7676 Woodbine Avenue, Markham, ON L3R 2N2, Canada

4 Department of Urologic Sciences, The University of British Columbia, 2775 Laurel Street, Vancouver, BC V5Z 1M9, Canada

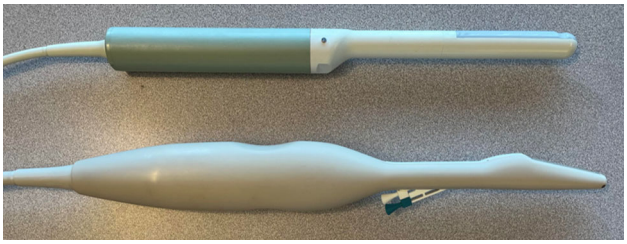

Fig. 1 An image showing the ExactVu microUS probe (bottom) compared to a traditional side-fire TRUS probe geometry (top). The traditional side-fire TRUS probe here is the E14CL4b endocavity biplane transducer (BK Medical, Herlev, Denmark)

ing the probe through known positions and combining the acquired images [6–10]. This should improve the registration performance by providing more spatial context.

Specific examples of these systems for prostate imaging include the use of a manually actuated (and mechanically tracked) 2D end-fire probe by Bax et al. [8] and mechanically actuated 2D side-fire probes by Aleef et al. [9] and Bax et al. [10]. These systems (and ones similar to them) have been used in robotic prostatectomy guidance [11] and brachytherapy seed placement [12].

MicroUS is a recent addition to the prostate imaging arsenal, particularly by using the ExactVu imaging system (Exact Imaging, Markham, Canada). This system uses a side-fire ultrasound (US) probe that can reach 29 MHz to image the prostate with a spatial resolution of 70 μm, which is approximately the size of prostatic ducts [13]. Meta-analyses have demonstrated that microUS is non-inferior to mpMRI for targeted prostate biopsy [14,15], and an upcoming trial will compare mpMRI fusion biopsy to targeted biopsy with microUS alone [16].

One limitation of the ExactVu system is that it can only acquire 2D images natively, and its unique probe geometry does not allow for the easy use of mechanical sweep systems which have been developed for other TRUS probes. As can be appreciated in Fig. 1, most TRUS probes are essentially cylindrical in shape, so that rotating the handle of the probe about its principal axis will also rotate the element array about that same axis, creating a 3D image with a well-defined geometry. The ExactVu microUS probe, on the other hand, does not have parallel axes between its handle and element array, so rotating about the handle's principal axis will result in an incorrect 3D image with incorrect spatial geometry.

The main contribution of this work is the ability to acquire reliable 3D microUS images, which will (i) allow for its inclusion in already-defined imaging workflows, such as 3D elastography [17], (ii) better facilitate MRI-to-US registration for fusion biopsies, (iii) allow for more accurate microUS-guided biopsies or brachytherapy without MRI for volumetric information, and (iv) serve as an important tool in robotic surgery guidance [11].

The objective of this paper is the design and validation of a novel robotically controlled system to generate accurate 3D images using the ExactVu microUS system.

The remainder of this paper outlines the design, fabrication, and validation of a robotically controlled system to generate accurate 3D microUS images using the ExactVu system, overcoming its geometric limitations.

Methods

System design

We follow the design approach for the robotic TRUS system [18] designed for other clinical ultrasound systems, which will allow us to leverage upon existing infrastructure that has been approved for previous in vivo studies [9].

The overall system is designed to be integrated with the clinical CIVCO EX-II stepper by replacing its native encoder with an external motor. This external motor is controlled by a control box which includes a microcontroller and is fitted with an optical encoder, ensuring accurate imaging increments.

To overcome the geometric challenges presented by the ExactVu probe's shape, we designed an adapter to align the probe with the robot such that the axis of rotation for the robot is parallel with the lateral direction of the ultrasound imaging array. The precise shape of the probe was determined using a Artec Leo handheld 3D scanner, which was post-processed and imported into the computer-aided design software Solidworks, where the adapter was created to align the axes based on the known angle between the center axis of the probe and the element array. The final design is shown in Fig. 2.

The device was created using an Afinia H800+ fused deposition modeling 3D printer and post-processed to ensure accurate alignment with the existing robotic TRUS system.

There is a 13 degree angle between the lateral direction of the element array of the probe and the principal axis of the handle. This information was used to choose the angle of our device. The center axis of the element array was then offset to be 3 mm above the center of rotation of the robotic system, so that it would travel along a circular path with a radius of 3 mm. This allows the system to maintain contact with the imaging surface, and thus maintain acoustic coupling.

The interface between our device and the probe was designed such that it affixes onto indentations in the handle of the probe, usually intended as an ergonomic grip. These indentations are on two sides of the device and are not identical. This design ensures that the probe can only be attached in one orientation and keeps it securely in place without requiring any adhesives or other modifications to the probe.

Scan conversion was performed in MATLAB R2022b (The Mathworks, Natick, MA, USA) to combine the series of

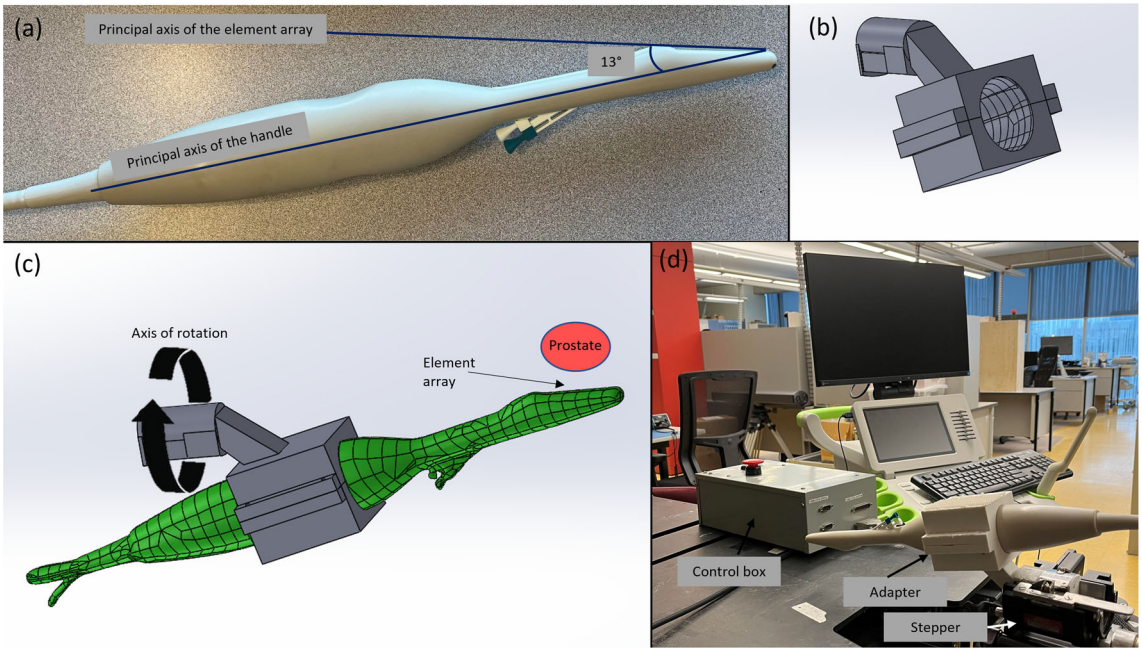

Fig. 2 A figure describing the design of this system. **a** An image of the ExactVu microUS probe, with the principle axes of the handle and element array defined, as well as the angle between them. **b** A view of the computer-aided design (CAD) model of our component without the microUS probe. **c** A screen capture of the CAD model of the ExactVu probe created by 3D scanning (green) and the component to transform the axis of rotation. **d** An image of the entire system

acquired 2D B-mode images into a single 3D volume using linear interpolation, with 0.2-mm isotropic pixel spacing. The increment between acquired 2D images was 1 degree. A block diagram of this system can be seen in Fig. 3.

System validation

Our system was validated using several methods, to ensure it created accurate 3D B-mode volumes. First, it underwent geometric validation in all three principal directions and then it was compared against a 3.0 T MRI scanner by imaging a commercial quality assurance prostate phantom, providing qualitative and quantitative results.

Geometric validation

Geometric validation of this imaging system was performed using a 3D printed fCal 2.1 phantom [19] which was strung with 20 μm diameter tungsten wire such that crossings were present with a known distance between each of them. This allows for a comparison between this known distance and what is measured in the reconstructed 3D microUS image, similar to the methods used to validate previous mechanical 3D US systems [6,7]. This phantom was imaged inside a water bath in several positions and orientations, so that measurements could be taken at various points in the imaging volume to form representative results. These images were acquired with an image depth setting of 50 mm. Due to the high frequency of this device, the maximum image depth is lower than in other systems because of the frequency-dependent amplitude attenuation coefficient (FDAAC), which is proportional to f^m, where f is the US imaging frequency and $1 < m < 2$ in soft tissue [20].

It is known from construction that wire crossings on the same row are 15 mm apart, while 5 mm separates rows, which can be seen in Fig. 4. The 3D reconstructed images were analyzed in 3D Slicer [21], with wire crossing locations manually confirmed and segmented by reviewing all three reconstructed planes and the volume rendered image. Euclidean distances were calculated between relevant points, and the absolute difference between this distance and the value known from construction (15 or 5 mm) represents our geometric validation error measurement.

A cartoon depiction of the approximate measurement locations is shown in Fig. 5 in two orthogonal projections.

For the purposes of this paper, the lateral, axial, and elevational directions will be used in reference to our image volume and will be defined with respect to the image plane in the center of our volume. These directions are also shown in Fig. 5.

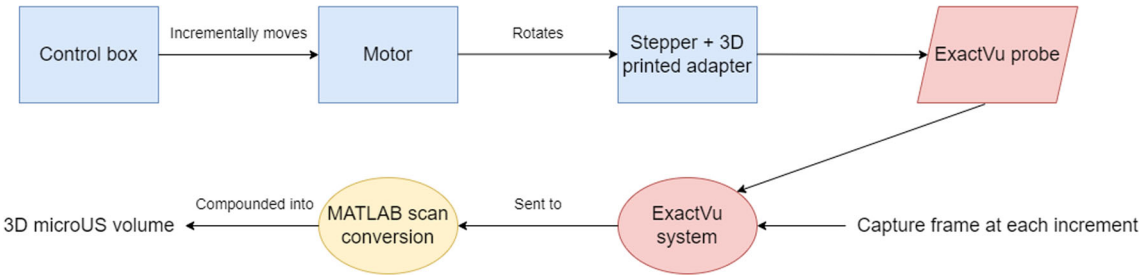

Fig. 3 A block diagram overviewing this 3D microUS system. Blue rectangles signify components which cause movement of the probe

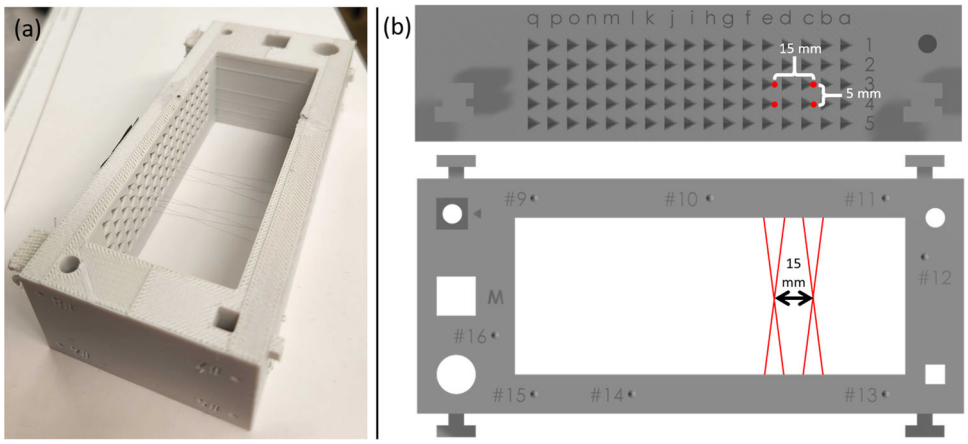

Fig. 4 An image showing the fCal phantom with crossings of 20 μm wire. The distance between crossings is known to be 15 mm within the same row, and 5 mm between rows by construction. **a** A photograph of the phantom. **b** Schematics showing the fCal phantom, the wire crossings and the distance between them in two projections

Phantom validation

Images were acquired of a commercial quality assurance prostate imaging phantom using our 3D microUS system and compared to images of the same phantom acquired with T_2-weighted MRI. Although mpMRI is used clinically to detect PCa, only T_2-weighted images were used here because we are only interested in the morphology of the phantom.

The phantom is a Tissue Equivalent Ultrasound Prostate Phantom 053 L (CIRS, Norfolk, VA, USA), which is intended for use with side-fire TRUS probes. This phantom includes several simulated anatomical features, including the rectal wall, seminal vesicles, urethra, and three simulated spherical lesions (each approximately 10 mm in diameter) inside the prostate. The dimensions of the prostate in this phantom are $5 \times 4.5 \times 4$ cm, and the overall phantom dimensions are $11.5 \times 7 \times 9.5$ cm.

The parameters of the microUS system were identical to those described above in the geometric validation procedure, while the T_2-weighted MRI image was acquired using a Philips Ingenia Elition 3T X (Philips Healthcare, Amsterdam, Netherlands), with voxel spacing of $1.5 \times 1.5 \times 1.5$ mm.

The 3D microUS and MRI image volumes were compared by first rigidly registering them using 3D Slicer, and then selecting representative images from all three reconstructed planes for qualitative comparison. For a quantitative comparison of our reconstructed image, the lesions in the phantom were manually segmented in both volumes, and the distances between the centroids of these segmentations were calculated in each image volume. These measurements were then compared between the two image volumes.

Results

Geometric validation

The results from our geometric validation are presented in Fig. 6, which demonstrates the sub-millimeter accuracy of our reconstructed 3D microUS images in all three dimensions. These results are further broken down into measurements taken in the near-field of the image (approximately 15–20 mm from the probe), and those taken when the wire crossings are in the far-field (approximately 35–40 mm from the probe). Overall, the mean geometric validation errors are 0.53, 0.17, and 0.30 mm in the elevational, lateral, and axial directions, respectively.

Phantom validation

Representative images of the prostate phantom from all three planes (transverse, sagittal, and coronal) of our reconstructed 3D microUS volume are compared to that of T_2-weighted

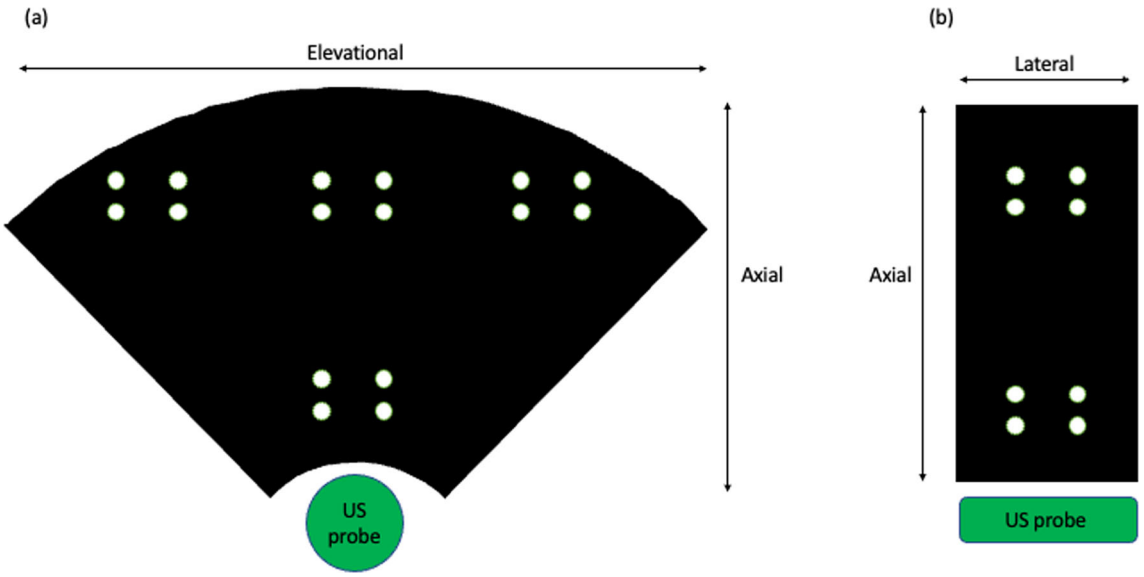

Fig. 5 A cartoon representation of the approximate measurement locations in projections of the image volume, showing **a** the elevational and axial directions, and **b** the lateral and axial directions

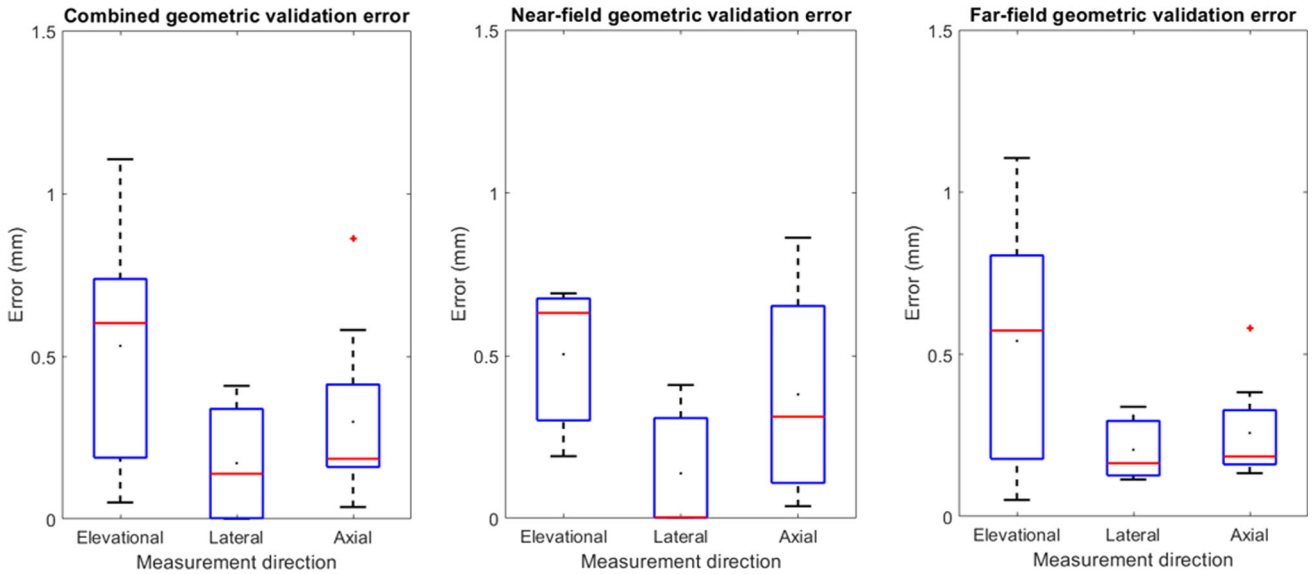

Fig. 6 A boxplot of the of the measured errors from our 3D microUS images of an fCal phantom whose wire crossings are known distance from each other by construction, showing the median and quartile values, with the mean values overlaid in black. The left plot shows all measurements combined, while the middle plot shows error measurements when the crossings are in the near-field (approximately 15–20 mm from the probe), and the right plot shows these measurements in the far-field (approximately 35–40 mm from the probe)

MRI after rigid registration in Fig. 7, demonstrating very good agreement.

The quantitative results of the comparison between the microUS and MRI volumes are shown in Table 1. The mean difference of the measurements between lesion centroids was 1.09 mm.

Discussion

The aim of this paper was to describe the design and validation of a novel method to acquire 3D microUS images using the ExactVu system, for use in prostate cancer biopsy guidance. This system was validated using a wire phantom, showing sub-millimeter error in all three reconstructed directions. There is anisotropy to the amount of error in the three directions, which is to be expected due to the different

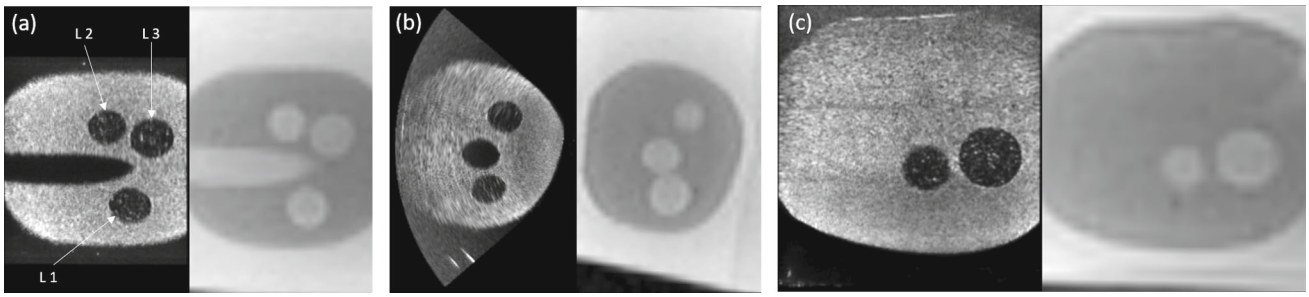

Fig. 7 A comparison between our reconstructed 3D microUS volume and T_2-weighted MRI images of the same prostate phantom after rigid registration, in **a** the coronal, **b** the transverse, and **c** the sagittal planes. **(a)** The lesions are each labeled as L1, L2, and L3, and these are used for the quantitative results in Table 1

Table 1 Quantitative results of microUS-to-MRI comparison

	MRI (mm)	MicroUS (mm)	Difference (mm)
L1-L2	21.24	19.84	1.51
L1-L3	18.58	17.09	1.40
L2-L3	11.41	11.05	0.37

amount of interpolation required in each direction. Although our geometric validation results show some error, they compare favorably to previously published standard values for US systems of 1.5 mm error in the in-plane vertical and horizontal directions (corresponding to axial and lateral here), and 2–3 mm in the elevational direction [7].

Results of the phantom validation demonstrate good agreement between our reconstructed volume and an image of the same phantom acquired using MRI, signifying that this system can lead to accurate imaging of anatomy at very high resolution in three dimensions. These results together indicate that our system can provide excellent anatomical information of the prostate in high resolution and three dimensions

This development method can be easily repeated for any TRUS system to acquire reliable 3D US volumetric imaging, provided the geometry of the probe is known and well-defined, namely the angle between the principal axes of the handle and element array and the offset between them.

Tracking the location of TRUS probes using electromagnetic tracking systems [22] allows the clinician to move the probe in a freehand fashion. Although this provides information regarding the location of each acquired frame, these frames will still likely create an irregular geometry, increasing the complexity of implementing image analysis algorithms such as 3D elastography [17].

Limitations

This study represents the initial validation and characterization of this 3D microUS system. Further refinements and validation will likely be required before it can be used clinically.

There were also potential sources of error in the construction and validation of this system. Namely, there are errors associated with the 3D scanner and 3D printer used here. Error from the 3D printer will be addressed in the future by fabricating the next generation of this system using more advanced techniques.

Some of the distance measurement error can also likely be accounted for by the differences in speed of sound between soft tissue and water, as argued in Ameri et al. [6], or the fact that the wire crossing points were manually determined, providing a source of human error.

Our quantitative phantom validation results are likely impacted by the relatively poor voxel spacing of our MRI volume, which would magnify any lesion centroid localization error arising from the manual segmentation.

Future work

This work represents a necessary step for extending the abilities of the ExactVu microUS system. The ability to image in 3D allows for the implementation of cutting-edge 3D elastography methods [17], improved mpUS methods for prostate biopsy guidance [23], or robotic surgery guidance [11]. Immediate next work includes refining the system so it can be used clinically, as well as implementing elastography using the ExactVu. We will also assess how these 3D image volumes can improve machine learning methods for cancer classification using the ExactVu [24].

Conclusion

This paper presents the design, construction, and validation of the first known system to capture robotically controlled 3D microUS images with the ExactVu system. Error was measured in all three principal directions of the image, show-

ing millimeter scale or better accuracy, and phantom images compared favorably to MRI. Future work will include using this development as a springboard to extend the utility of this microUS system to leverage microUS' inherent advantages over traditional US, including superior spatial resolution.

Acknowledgements This work was funded with a Natural Sciences and Engineering Research Council Canada Graduate Scholarship—Doctoral and the C.A. Laszlo Chair held by Professor Salcudean.

Declarations

Conflict of interest All authors declare that they have no competing interests. Brian Wodlinger is employed by Exact Imaging.

References

1. Sung H, Ferlay J, Siegel RL, Laversanne M, Soerjomataram I, Jemal A, Bray F (2021) Global cancer statistics 2020: Globocan estimates of incidence and mortality worldwide for 36 cancers in 185 countries. CA Cancer J Clin 71(3):209–249
2. Izawa JI, Klotz L, Siemens DR, Kassouf W, So A, Jordan J, Chetner M, Iansavichene AE (2011) Prostate cancer screening: Canadian guidelines 2011. Can Urol Assoc J 5(4):235
3. Onur R, Littrup PJ, Pontes JE, Bianco FJ Jr (2004) Contemporary impact of transrectal ultrasound lesions for prostate cancer detection. J Urol 172(2):512–514
4. Serefoglu EC, Altinova S, Ugras NS, Akincioglu E, Asil E, Balbay D (2013) How reliable is 12-core prostate biopsy procedure in the detection of prostate cancer? Can Urol Assoc J 7(5–6):e293-8
5. Wegelin O, Exterkate L, van der Leest M, Kummer JA, Vreuls W, de Bruin PC, Bosch JR, Barentsz JO, Somford DM, van Melick HH (2019) The future trial: a multicenter randomised controlled trial on target biopsy techniques based on magnetic resonance imaging in the diagnosis of prostate cancer in patients with prior negative biopsies. Eur Urol 75(4):582–590
6. Ameri G, Barker K, Sham D, Fenster A (2020) Mechanically-assisted 3D ultrasound scanner for urogynecological applications: preliminary results, vol 11319, pp 161–166 SPIE
7. Neshat H, Cool DW, Barker K, Gardi L, Kakani N, Fenster A (2013) A 3D ultrasound scanning system for image guided liver interventions. Med Phys 40(11):112903
8. Bax J, Cool D, Gardi L, Knight K, Smith D, Montreuil J, Sherebrin S, Romagnoli C, Fenster A (2008) Mechanically assisted 3D ultrasound guided prostate biopsy system. Med Phys 35(12):5397–5410
9. Aleef TA, Zeng Q, Morris WJ, Mahdavi SS, Salcudean SE (2022) Registration of trans-perineal template mapping biopsy cores to volumetric ultrasound. Int J Comput Assist Radiol Surg 17(5):929–936
10. Bax J, Smith D, Bartha L, Montreuil J, Sherebrin S, Gardi L, Edirisinghe C, Fenster A (2011) A compact mechatronic system for 3D ultrasound guided prostate interventions. Med Phys 38(2):1055–1069
11. Samei G, Tsang K, Kesch C, Lobo J, Hor S, Mohareri O, Chang S, Goldenberg SL, Black PC, Salcudean S (2020) A partial augmented reality system with live ultrasound and registered preoperative MRI for guiding robot-assisted radical prostatectomy. Med Image Anal 60:101588
12. Hrinivich WT, Hoover DA, Surry K, Edirisinghe C, Montreuil J, D'Souza D, Fenster A, Wong E (2017) Simultaneous automatic segmentation of multiple needles using 3D ultrasound for high-dose-rate prostate brachytherapy. Med Phys 44(4):1234–1245
13. Dias AB, O'Brien C, Correas J-M, Ghai S (2022) Multiparametric ultrasound and micro-ultrasound in prostate cancer: a comprehensive review. Br J Radiol 95(1131):20210633
14. Sountoulides P, Pyrgidis N, Polyzos SA, Mykoniatis I, Asouhidou E, Papatsoris A, Dellis A, Anastasiadis A, Lusuardi L, Hatzichristou D (2021) Micro-ultrasound-guided vs. multiparametric magnetic resonance imaging-targeted biopsy in the detection of prostate cancer: a systematic review and meta-analysis. J Urol 205(5):1254–1262
15. You C, Li X, Du Y, Peng L, Wang H, Zhang X, Wang A (2022) The microultrasound-guided prostate biopsy in detection of prostate cancer: A systematic review and meta-analysis. J Endourol 36(3):394–402
16. Klotz L, Andriole G, Cash H, Cooperberg M, Crawford ED, Emberton M, Gomez-Sancha F, Klein E, Lughezzani G, Marks L, Montorsi F, Salomon G, Sanchez-Salas R, Shore N, Taneja S (2022) Optimization of prostate biopsy-micro-ultrasound versus MRI (optimum): A 3-arm randomized controlled trial evaluating the role of 29 mhz micro-ultrasound in guiding prostate biopsy in men with clinical suspicion of prostate cancer. Contemp Clin Trials 112:106618
17. Zeng Q, Honarvar M, Schneider C, Mohammad SK, Lobo J, Pang EH, Lau KT, Hu C, Jago J, Erb SR, Rohling R, Salcudean SE (2020) Three-dimensional multi-frequency shear wave absolute vibro-elastography (3D s-wave) with a matrix array transducer: implementation and preliminary in vivo study of the liver. IEEE Trans Med Imaging 40(2):648–660
18. Adebar T, Salcudean S, Mahdavi S, Moradi M, Nguan C, Goldenberg L (2011) A robotic system for intra-operative trans-rectal ultrasound and ultrasound elastography in radical prostatectomy. Springer, pp 79–89
19. Lasso A, Heffter T, Rankin A, Pinter C, Ungi T, Fichtinger G (2014) Plus: open-source toolkit for ultrasound-guided intervention systems. IEEE Trans Biomed Eng 61(10):2527–2537
20. Dance D, Christofides S, Maidment A, McLean I, Ng K (2014) Diagnostic radiology physics. Int Atom Energy Agency 299
21. Kikinis R, Pieper SD, Vosburgh KG (2014) In3d slicer: a platform for subject-specific image analysis, visualization, and clinical support. Springer, pp 277–289
22. Lugez E, Sadjadi H, Joshi CP, Hashtrudi-Zaad K, Akl SG, Fichtinger G (2019) Field distortion compensation for electromagnetic tracking of ultrasound probes with application in high-dose-rate prostate brachytherapy. Biomed Phys Eng Exp 5(3):035026
23. Rohrbach D, Wodlinger B, Wen J, Mamou J, Feleppa E (2018) High-frequency quantitative ultrasound for imaging prostate cancer using a novel micro-ultrasound scanner. Ultrasound Med Biol 44(7):1341–1354
24. Shao Y, Wang J, Wodlinger B, Salcudean SE (2020) Improving prostate cancer (PCA) classification performance by using three-player minimax game to reduce data source heterogeneity. IEEE Trans Med Imaging 39(10):3148–3158